Insulator-conductor behavior of a two-dimensional electron system on a helium film

Cláudio José da Silva,[1] José Pedro Rino,[1,*] and Ladir Cândido[2]
[1]*Departamento de Física, Universidade Federal de São Carlos, São Carlos, 13.565-905 São Carlos, SP, Brazil*
[2]*Instituto de Física, Universidade Federal de Goiás, Goiânia, 74.001-970 Goiânia, GO, Brazil*
(Received 19 December 2007; published 7 April 2008)

We performed a Langevin molecular dynamics simulation to study the response of a two-dimensional (2D) constrained electron system on a helium film due to an external force parallel to the surface. The electron drift velocity was obtained as a function of the driven force for different values of film thickness and dielectric constants of the substrate in the low temperature regime ($T \rightarrow 0$). We observed that the system had undergone an insulator-conductor transition after a finite depinning threshold of the driven force. This should be helpful for understanding the nonlinear dc conductivity observed in 2D systems, such as that in semiconductor heterostructures.

DOI: 10.1103/PhysRevB.77.165407 PACS number(s): 71.10.−w, 52.65.Yy, 71.30.+h

I. INTRODUCTION

The study of low dimensionality is a central task of modern condensed matter physics and has sharply risen. Two-dimensional (2D) Coulomb systems have greatly contributed to developments in fundamental physics. Some typical and important examples are electrons in semiconductor structures and electrons floating on a liquid helium surface. The former are important for understanding phenomena such as the fractional quantum Hall effect[1] and 2D metal-insulator transitions.[2] The latter have been promising candidates to a set of strongly correlated quantum bits in quantum computers.[3] They are unique and provide an ideal system for experimental and theoretical research due to their exceptional uniformity and cleanliness. Furthermore, at low enough temperatures and densities, the system undergoes a transition known as the Wigner crystallization,[4] in which the electrons avoid each other by arranging themselves on a triangular lattice. The Wigner crystal can also be induced in denser systems considering thin layers (typically $\sim$100 Å) of liquid helium covering a solid substrate or by subjecting the 2D electrons to strong perpendicular magnetic fields.[5]

Electrons on helium film offer many interesting possibilities to understand electron mobility, conduction properties, polaronic effects on the mobility, complex charge, etc.[6] The conduction properties of a pinned electron crystal become an ideal system in which one can test experimental observations of nonlinear behavior of the current-voltage $I(V)$ on two-dimensional semiconductor heterojunctions.[7] The advantage in studying this analogous system with electrons on a helium film is that the interaction with the substrate can be modified by varying only the film thickness. The surface electronic mobility in many situations is affected by impurities or by the surface profile of the substrate beneath the helium film. Experimental results on sliding charge-density waves,[8] magnetically induced Wigner solid,[9] and magnetoconductivity[10] have shown the importance of the disorder and pinning on the nonlinear response of the system to an external driven force. Also, numerical results for the flux pinning model in type-II superconductors,[11] dynamical Wigner crystal with charged impurities on the underlying substrate,[12] moving disordered vortex lattice,[13] and depinning on quasi-one-dimensional systems[14] give us a good qualitative description of such phenomena.

In the present paper, we use Langevin molecular dynamics simulation to describe the behavior of a two-dimensional classical electron lattice on a helium film supported by a dielectric substrate when it is driven by an external force. In the simulation, a perfect sliding crystal is obtained if an external electric field is applied parallel to the surface. This occurs because the interaction energy of the surface deformation (dimples) is very small compared to the average Coulomb energy, and the appearance of the dimple lattice practically has no effect on the pinned lattice. The static deformation of the helium surface just accompanies the Wigner crystal. Also, the substrate is considered perfectly flat since an accurate description of the effect of the substrate irregularities requires knowledge of the interaction of bound electrons with an uneven interface, and this is not trivial. The image charges of the electrons produced inside the helium and in the substrate do not pin the crystal since they are not quenched. Therefore, to simulate a pinned crystal, we consider an in-plane constriction potential with a Lorentzian shape centered at the origin, which behaves as a barrier to the motion of electrons.[15]

We report the influence on the electron drift velocity, which is driven by an external electric field and constrained by a Lorentzian barrier, as a function of the film thickness and substrate. This assumption was inspired by recent experimental dc measurements of electrons on a liquid helium film.[16,17] Also, the theoretical proposal to create quantum dots on a helium surface[18] by using electrodes submerged into the helium to locally confine the electrons has motivated us to simulate such a constriction. Similar pinning models have been used in a quasi-one-dimensional system.[14] Notwithstanding, the kind of electron flow reported in this work is similar to those that appear in dusty plasma crystals in a flowing plasma.[19,20] However, it is out of the scope of this work to extend our results to those systems. Our calculations were carried out at a very low temperature regime ($T \rightarrow 0$).

The paper is organized as follows. In Sec. II, we describe the system and the procedure we have used in the Langevin dynamics. In Sec. III, we discuss our results. We conclude in Sec. IV.

II. MODEL AND SIMULATION PROCEDURE

Our system consists of N electrons deposited on a helium film with dielectric constant ϵ and thickness d located over a solid substrate with dielectric constant ϵ_s. The interaction potential between two electrons on the surface is given by[21]

$$V_{ee}(r) = e^{*2}\left[\frac{1}{r} - \frac{\delta}{\sqrt{r^2 + (2d)^2}}\right], \tag{1}$$

where $e^* = e/\sqrt{(1+\epsilon)/2}$ is the electron charge renormalized due to the screening of the electron-electron interaction by the substrate and $\delta = (\epsilon_s - \epsilon)/(\epsilon_s + \epsilon)$. A helium film covering a metallic substrate ($\epsilon_s \to \infty$) represents an extreme example of such screening. In this case, the electrons interact via the dipole potential $V_{ee}(r) \to 2e^2d^2/r^3$ if $d \ll r$.

To obtain a pinned electron lattice, we consider a two-dimensional Lorentzian shape potential centered at the origin. Therefore, the interaction between one electron and the constriction is given by

$$V_{ec}(x,y) = \frac{V_0}{1 + \alpha^2x^2 + \beta^2y^2}, \tag{2}$$

where $(x,y) \equiv r$ is the position of the electron and V_0 is the maximum of the constriction. A positive (negative) V_0 will result in a barrier (valley) in the center of the system, whose strength produces a local disorder in the lattice.

A positive background is imposed in order to guarantee a charge neutrality of the system. Its energy contribution U_b is summed to the total potential energy, which is given by

$$U = \frac{e^{*2}}{2}\sum_{i\neq j}^{N}\left[\frac{1}{r_{ij}} + \frac{\delta}{\sqrt{r_{ij}^2 + (2d)^2}}\right] + \sum_{i=1}^{N}\frac{V_0}{1 + \alpha^2x_i^2 + \beta^2y_i^2} + U_b, \tag{3}$$

where $r_{ij} = |\vec{r}_i - \vec{r}_j|$. To take into account the long-range character of Coulomb interactions, we have used the Ewald summation. The system consists of N electrons in a rectangular box of area $A = L_xL_y$, such that $L_x = L_y\sqrt{3}/2$, with periodic boundary conditions to eliminate surface effects. We have concentrated the calculations on three values of the areal electron density, e.g., 1.477×10^8, 2.2×10^9, and 1.3×10^{10} cm^{-2}, corresponding to typical experimental data, even though we have verified that the threshold value of the external force does not depend on the density. Also, most of the results shown in this paper are for a system with $d = 100$ Å, $\delta = 0.5789$, and $N = 400$ electrons. Checks with up to 784 electrons did not change the results (within the statistical error).

Another important requirement that is adopted in the simulation is to write down a suitable set of units to rewrite all variables of the problem. Then, we have assumed that the parameters $\sqrt{A}$ and $E_0 = e^2/2\sqrt{A}$ are in units of length and energy, respectively. With this assumption, the constriction potential parameters should be rewritten as $V_0^* = E_0V_0$, $\alpha^* = \sqrt{A}\alpha$, and $\beta^* = \sqrt{A}\beta$. Also, the units of time and temperature are $\tau = \sqrt{mA/2E_0}$ and $T_0 = E_0/k_B$, respectively, where k_B is the Boltzmann constant. One may also use as a unit of length the typical interelectron spacing r_0, which is proportional to the areal electron density $n_s = 1/\pi r_0^2$.

To consider the effect of an external force, we couple the system to a heat bath described by the Langevin equation of motion,[22]

$$m\frac{d^2\vec{r}}{dt^2} = -\nabla U(r) - \gamma m\frac{d\vec{r}}{dt} + \vec{\xi}(t), \tag{4}$$

where γ controls the frictional drag on the motion of the particles and $\vec{\xi}(t)$ is the random force vector, which has zero average $\langle\vec{\xi}_i(t)\rangle = 0$, and its standard deviation must be written as

$$\langle\vec{\xi}_i(t)\vec{\xi}_j(t')\rangle = 2m\gamma k_BT\delta_{ij}\delta(t - t'). \tag{5}$$

The external driven force f acts only in the x direction; therefore, Langevin's equations of motion are given by

$$m\frac{d^2x_i}{dt^2} = -\gamma m\frac{dx_i}{dt} - \frac{\partial U}{\partial x_i} + \xi_{ix}(t) + f,$$

$$m\frac{d^2y_i}{dt^2} = -\gamma m\frac{dy_i}{dt} - \frac{\partial U}{\partial y_i} + \xi_{iy}(t). \tag{6}$$

To fulfill the dimensionless criterion, we must use $\xi_0 = f_0 = m\sqrt{A}\tau^2$ as the unit of the random and driven forces. The friction coefficient is measured in units of $\gamma_0 = 1\tau$.

The typical value of γ obtained in dusty plasma experiments lies between 0.1 and 1.0 for the weak Coulomb coupling limit.[23] Since we have considered a pure Coulomb potential and a higher constriction potential compared to the system size, it is necessary to consider a large value of the friction coefficient to ensure the stability of the system and to keep the temperature constant. Thus, in our simulations, we have estimated γ to be between 5.0 and 20.0, and in our dimensionless unit, it ranges from $\gamma^* \sim 1.107 \times 10^3$ to 1.243×10^4. All of the results shown here were obtained for a single value of the friction coefficient, i.e., $\gamma^* = 1.0 \times 10^4$.

To integrate Langevin's equations of motion above, we use the BBK integrator,[24] which has the following form:

$$v\left(t + \frac{1}{2}\Delta t\right) = \left(1 - \frac{1}{2}\gamma\Delta t\right)v(t) + \frac{1}{2}\Delta t\{-\nabla U[r(t)] + R(t)\},$$

$$r(t + \Delta t) = r(t) + \Delta t v\left(t + \frac{1}{2}\Delta t\right),$$

$$v(t + \Delta t) = \frac{1}{1 + \frac{1}{2}\gamma\Delta t}\left(v\left(t + \frac{1}{2}\Delta t\right) + \frac{1}{2}\Delta t\{-\nabla U[r(t + \Delta t)] + R(t + \Delta t)\}\right),$$

where

$$R(t) = \sqrt{\frac{2\gamma k_BT}{\Delta t}}Z(t), \tag{7}$$

and $Z(t)$ represents a vector of independent Gaussian random numbers with mean zero and variance one.

Before taking into account the effect of the external field on the system, we must obtain the ground state configura-

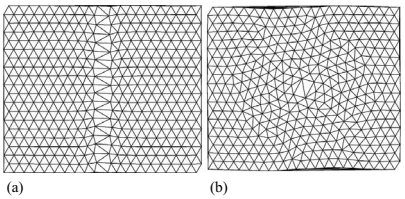

FIG. 1. Delaunay triangulation for a triangular lattice with 400 electrons. The maximum value of the constriction in this case is $V_0^*=60$ with (a) $\alpha^*=30$ and $\beta^*=2$, and (b) $\alpha^*=\beta^*=20$.

tions resulting from the competition between the Coulomb interaction and the Lorentzian potential that constrains the motion of the electrons on the plane. This was done for different numbers of particles and constriction parameters. First, we used the Metropolis Monte Carlo (MC) method[25] to obtain an equilibrium configuration at some finite temperature T after carrying out 10^5 MC steps. Second, the $T=0$ equilibrium configurations were obtained by the simulated annealing technique,[26] by heating up the system to a high temperature and then cooling it down to a low temperature. Once the initial electron configuration was attained, the external force was slowly applied.

In all calculations, we used a time integration step of $\Delta t^*=1.34\times10^{-3}$. The averages are collected after 5×10^5 time steps. For each increment of the driven force, we allowed the system to reach equilibrium with the same amount of time steps.

III. RESULTS AND DISCUSSION

We first investigated the ground state configurations, which should no longer be a perfect triangular lattice. The local disorder in the electron lattice that arises from the interplay between the strong Coulomb repulsion and the constriction potential in the middle of the system is shown in Fig. 1 by means of the Delaunay triangulation.

In this work, we report only the results considering a positive constriction. The shape of the barrier created by the constriction depends on the parameters α^* and β^*. For $\beta^*=0$, we have a wall in the y direction and the motion of the electrons is possible only over the barrier. Therefore, there is a strong dependence of the depinning threshold on the value of V_0^*. In Fig. 1(a), we show the effect of the constriction with $\alpha^*>\beta^*$ (namely, $\alpha^*=30$ and $\beta^*=2$). One can observe a smoother disorder only at the edges of the system near the constriction, and if an external force is applied, the electrons mainly flow through these edges. However, for a high driven force, they can also flow over the constriction. In Fig. 1(b), we show the Delaunay triangulation for $\alpha^*=\beta^*$; this condition causes a weak local disorder and the depinning is more likely to occur in the system since the electrons initially move around the constriction. In most calculations, we analyzed only the case shown in Fig. 1(a), with the following constriction parameters: $V_0^*=60$, $\alpha^*=30$, and $\beta^*=2$.

The main focus of our work is the drift electron velocity, which is analogous to an electrical current when the system is in the presence of a parallel electric field. Here, we consider an external driven force to simulate this field. This drift velocity along the x direction is measured as

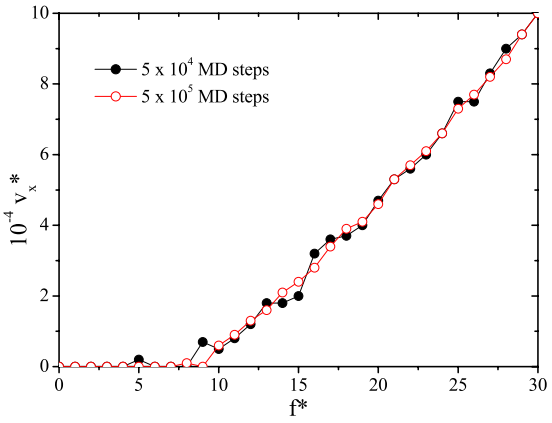

FIG. 2. (Color online) Average electron velocity versus driven force for two molecular dynamics runs with different number of steps.

$$v_x=\frac{1}{N}\sum_{i=1}^{N}\vec{v}_i\cdot\hat{x}, \tag{8}$$

where the average was taken at each force increment and over the whole time integration. Figure 2 shows the simulated result of v_x^* versus f^* for the film on a glass substrate ($\delta=0.5789$). Note that there is a critical pinning force f_c^* (≈9). For values of f_c^* below this depinning, the lattice is pinned by the constriction and there is no net motion. This kind of dynamic response clearly indicates an insulated state of the electron lattice below a driven threshold. After a sudden jump on the velocity, the lattice becomes a conductor.

It is important to stress that the number of time steps is crucial for a good average on the drift velocity. This is also shown in Fig. 2, in which we consider two different numbers of time steps for integration, e.g., 5×10^4 and 5×10^5 steps. A long time evolution is needed to allow the particles to travel throughout the whole system. Otherwise, some electrons could make a quick path and should not overcome the constriction barrier. As a result, this would provide trace counts with poor statistics for the drift velocity on the depinning threshold. Note that the more f^* increases, the more the two curves become very similar because the motion of the electrons becomes more ordered and they tend to coherently move along the x direction.

The influence of the constriction maximum on the depinning is shown in Fig. 3. In the case of a weak pinning, the response of the lattice to an external force is basically linear and the electrons begin to flow in channels above f_c^*, which produce a nonplastic depinning, once all the particles move together. The inset in Fig. 3 shows that when the pinning starts to increase, the v-f curve begins to deviate from linear behavior. This is similar to the dynamic response on charge-density waves at a weak pinning.[27] For a strong pinning (high value of V_0), some electrons are reflected by the constriction and become trapped near the barrier. In this case, the depinning is essentially plastic. This kind of depinning can

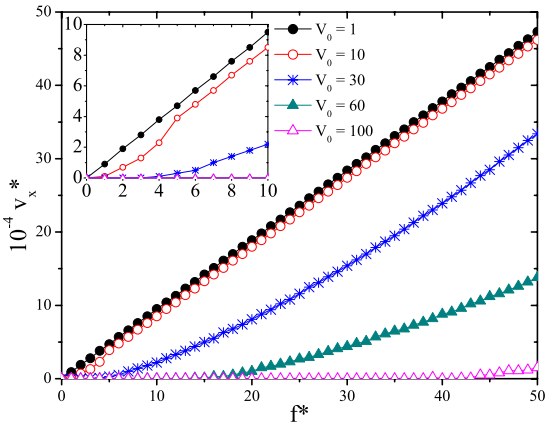

FIG. 3. (Color online) Drift velocity of electrons as a function of external driven force for some values of the constriction's maximum. The inset shows an amplification of the region of weak driven force.

be understood by means of the critical behavior near the threshold, which is obtained by using the scaling relation $v=[(f-f_c)/f_c]^{\xi}$, where ξ is the critical exponent. In Fig. 4, we show the scaling fit for some values of the constriction maximum. One can observe the transition between the two regimes of depinning (e.g., the change in the slope: from solid circle to solid up triangle). For both nonplastic and plastic regimes, the values of critical exponents are in agreement with the predicted values.[27,28]

It is well known that when the distance between the electron layer and the substrate is smaller than the average interparticle distance r_0, the Coulomb interaction becomes $V_{ee}(r)=e^2(1-\delta)/r+2\delta e^2d^2/r^3$. This implies that for a metallic substrate ($\delta=1$), the interaction is dipolarlike.[21] On the other hand, if $d \gg r_0$, the screening due to the substrate is negligible and the interaction is essentially Coulombic, i.e., $V_{ee}(r)=e^2/r$. Therefore, we can now analyze the influence of the film thickness and the substrate on the drift velocity of the electrons. In Fig. 5(a), we report the v_x^*-f^* curve for several values of d. Note that the critical value of f^* decreases with increasing d and the system more rapidly becomes a

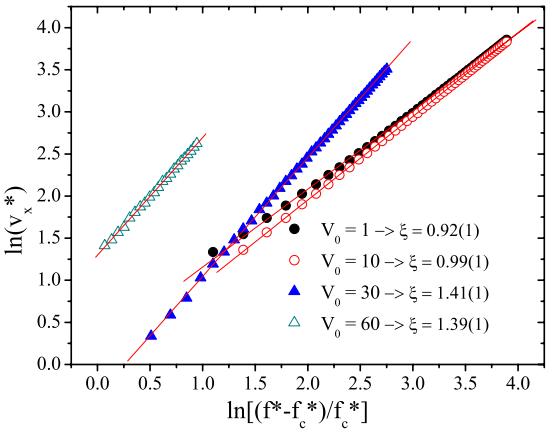

FIG. 4. (Color online) Scaling behavior near the threshold for some values of the constriction maximum.

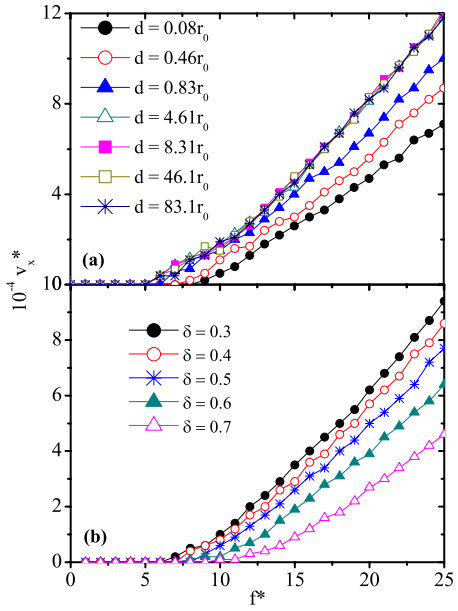

FIG. 5. (Color online) Drift velocity of electrons as a function of external driven force for different (a) film thicknesses and (b) substrates.

conductor. This is a coherent result since the electron-electron interaction becomes stronger than the electron constriction and when the system reaches the bulk limit ($d \gg r_o$), the depinning threshold does not vary anymore.

Such an effect of the screening can also be seen in Fig. 5(b), in which we show the velocity-driven force dependence for some values of δ for a film thickness of 100 Å. We observe that as the screening increases ($\delta \rightarrow 1$), the depinning threshold increases too, which indicates that the Coulomb interaction becomes less pronounced than the constriction potential. The critical exponent for $\delta=0.7$ was estimated as $\xi=1.57(2)$. This confirms the plastic flow for a strong pinning force. Our results for the critical exponents in the plastic regime are in good agreement with the experimental observation and theoretical prediction for transport phenomena in metallic quantum dots.[29]

Finally, we observed the phenomenon of dynamic reordering in our system. This can be seen in Fig. 6, in which we illustrate the electron trajectories for a system that contains $N=256$ electrons constrained by a potential with $V_0^*=50$, $\alpha^*=20$, and $\beta^*=2$. In this case, the system evolves for only 5×10^4 time steps for each value of f^* because if the trajectories are taken over a long time integration, the electron flow appears everywhere in the system, despite the fact that most electrons flow in some preferred paths.

When the driving force is increased, the electrons remain pinned, as shown in Fig. 6(a), until a certain critical value of the force is reached, when the electrons begin to move, trying to overcome the constriction. Figure 6(b) shows that, initially, they flow in crossing channels that are mainly in the border of the system near the barrier. Figures 6(c) and 6(d) indicate that for high values of the force, the interconnecting channels undergo a gradual reordering and the system starts to move in an ordered channel structure. This kind of flow

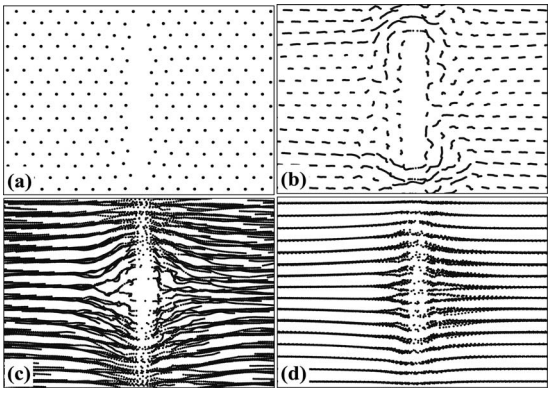

FIG. 6. Electron trajectories at increasing driving forces for a system with $N=256$, $n_s=1.3\times10^{10}$ cm^{-2}, $\delta=0.5789$, $V_0^*=50$, $\alpha^*=20$, and $\beta^*=2$. $f_c^*=$(a) 1.0, (b) 10.0, (c) 50.0, and (d) 100.0.

signals that our system also indicates a universal character of the dynamic reordering, which has been extensively studied in a great variety of systems.[30]

IV. CONCLUSIONS

In this work, we studied a two-dimensional system of electrons on a helium film adsorbed on a substrate subject to an external electric field by means of Langevin dynamics simulation. We examined the influence of the thickness of the film and the kind of substrate on the drift electron velocity. The system was constrained by an in-plane potential with a Lorentzian shape that simulates a pinning center. We have observed that the drift velocity of electrons showed a depinning threshold as the external force increased, which characterizes an insulator-conductor transition. Furthermore, when the film thickness was increased, the critical depinning force decreased down to the bulk limit. When the dielectric constant of the substrate increased, it became harder for the system to undergo a depinning. Such results are very encouraging and they may be helpful for understanding the influence of the surrounding medium on the metal-insulator transition in two dimensions more clearly.

ACKNOWLEDGMENTS

The authors would like to thank the Coordenação de Aperfeiçoamento de Pessoal de Nível Superior (CAPES), the Conselho Nacional de Desenvolvimento Científico e Tecnológico (CNPq), and the Fundação de Amparo à Pesquisa do Estado de São Paulo (FAPESP) for financial support. L.C. also thanks FUNAPE-GO for partial support.

*djpr@df.ufscar.br

[1] D. C. Tsui, H. L. Stormer, and A. C. Gossard, Phys. Rev. Lett. **48**, 1559 (1982).
[2] S. V. Kravchenko and M. P. Sarachik, Rep. Prog. Phys. **67**, 1 (2004).
[3] P. M. Platzman and M. I. Dykman, Science **284**, 1967 (1999).
[4] E. Wigner, Phys. Rev. **46**, 1002 (1934).
[5] D. S. Fisher, Phys. Rev. B **26**, 5009 (1982).
[6] Y. Monarkha and K. Kono, *Two-Dimensional Coulomb Liquids and Solids* (Springer, Berlin, 2004).
[7] V. J. Goldman, M. Santos, M. Shayegan, and J. E. Cunningham, Phys. Rev. Lett. **65**, 2189 (1990).
[8] H. W. Jiang and A. J. Dahm, Phys. Rev. Lett. **62**, 1396 (1989).
[9] F. I. B. Williams, P. A. Wright, R. G. Clark, E. Y. Andrei, G. Deville, D. C. Glattli, O. Probst, B. Etienne, C. Dorin, C. T. Foxon, and J. J. Harris, Phys. Rev. Lett. **66**, 3285 (1991).
[10] A. Kristensen, K. Djerfi, P. Fozooni, M. J. Lea, P. J. Richardson, A. Santrich-Badal, A. Blackburn, and R. W. van der Heijden, Phys. Rev. Lett. **77**, 1350 (1996).
[11] H. J. Jensen, A. Brass, and A. J. Berlinsky, Phys. Rev. Lett. **60**, 1676 (1988).
[12] C. Reichhardt, C. J. Olson, N. Gronbech-Jensen, and Franco Nori, Phys. Rev. Lett. **86**, 4354 (2001).
[13] Y. Cao and Z. Jiao, Physica C **387**, 341 (2003).
[14] G. Piacente and F. M. Peeters, Phys. Rev. B **72**, 205208 (2005).
[15] R. Chitra, T. Giamarchi, and P. Le Doussal, Phys. Rev. B **65**, 035312 (2001).
[16] J. Klier, I. Doicescu, and P. Leiderer, J. Low Temp. Phys. **121**, 603 (2000).
[17] V. Shikin, J. Klier, I. Doicescu, A. Würl, and P. Leiderer, Phys. Rev. B **64**, 073401 (2001).
[18] M. I. Dykman, P. M. Platzman, and P. Seddighrad, Physica E (Amsterdam) **22**, 767 (2004).
[19] D. Samsonov, J. Goree, Z. W. Ma, A. Bhattacharjee, H. M. Thomas, and G. E. Morfill, Phys. Rev. Lett. **83**, 3649 (1999).
[20] V. A. Schweigert, I. V. Schweigert, V. Nosenko, and J. Goree, Phys. Plasmas **9**, 4465 (2002).
[21] L. Candido, J. P. Rino, and N. Studart, Phys. Rev. B **54**, 7046 (1996).
[22] J. Albers, J. M. Deutch, and I. Oppenheim, J. Chem. Phys. **54**, 3541 (1971); J. M. Deutch and I. Oppenheim, *ibid.* **54**, 3547 (1971).
[23] D. Winske and M. Rosenberg, IEEE Trans. Plasma Sci. **26**, 92 (1998).
[24] A. Brunger, C. L. Brooks III, and M. Karplus, Chem. Phys. Lett. **105**, 495 (1984).
[25] N. Metropolis, A. W. Rosenbluth, M. N. Rosenbluth, and A. H. Teller, J. Chem. Phys. **21**, 1087 (1953).
[26] S. Kirkpatrick, C. D. Gelatt, and M. P. Vecchi, Science **220**, 671 (1983).
[27] D. S. Fisher, Phys. Rev. B **31**, 1396 (1985).
[28] M. C. Miguel, J. S. Andrade, Jr., and S. Zapperi, Braz. J. Phys. **33**, 557 (2003).
[29] C. Kurdak, A. J. Rimberg, T. R. Ho, and J. Clarke, Phys. Rev. B **57**, R6842 (1998).
[30] C. Reichhardt, C. J. Olson, I. Martin, and A. R. Bishop, Europhys. Lett. **61**, 221 (2003).